Progress In Electromagnetics Research M, Vol. 67, 9–19, 2018

Channel Characterization of Circularly Polarized Antenna MIMO System in an Underground Mine

Moulay El Hassan El Azhari[1, *], Larbi Talbi[1], Lamia Arabi[2], Mourad Nedil[2], Mohamed L. Seddiki[2], and Nahi Kandil[2]

Abstract—In this paper, a channel characterization of an RF link using circularly polarized antennas inside a mine is performed. The association of circular polarization with multiple-input-multiple-output (MIMO) radio technologies represents a powerful tool to improve the performance of an underground RF channel. The statistical parameters of the channel are derived from in-mine measurements at the 2.4 GHz band for both co-polarization (CP) and cross-polarization (XP) scenarios. Results show a remarkable improvement through the use of MIMO combined with circular polarization compared to the regular patch MIMO antenna system, in terms of channel capacity and path loss. This improvement increases significantly at the XP scenarios, reaching up to 18 bps/Hz for channel capacity and up to 21 dB for path loss. The RMS delay spread for a circularly polarized setup is generally higher than the linearly polarized MIMO patch setup due to surface roughness of the gallery. In the linear polarization case, a signal degradation of more than 15 dB at the XP case is observed compared to the CP scenario. This signal loss that is due to depolarization is somewhat mitigated by the surface roughness. Due to its superior and stable performance, MIMO combined with circular polarization is better suited than a regular MIMO patch system for in-mine uses especially in the applications where the transmitter may change direction with respect to the receiver.

1. INTRODUCTION

The channel propagation allows the flow of information by means of electromagnetic waves which propagate in the environment and are emitted or captured by antennas. However, in underground mines, the environment is composed of barriers that disturb the transmission of information through physical effects like reflection, diffraction and scattering. To combat these potentially damaging phenomena, the properties of the propagation channel (taking into account the effects of the environment on electromagnetic waves) should be known with precision. The channel characterization aims to quantify these properties through the derivation of important channel parameters, namely, the impulse response, Root Mean Square (RMS) delay spread, Rican k-factor, and path loss (PL) exponent.

Driven by an increasing pressure to improve mining conditions by applying reliable underground communication systems [1], the research community has multiplied efforts in studying wireless communication in underground mines. The aim is to replace the wired communication link which requires expensive maintenance and has limited scalability [2] by a reliable and safe wireless link. These links are essential for monitoring underground mines and launching a rescue operation in the case of an accident, hence insuring personnel safety and saving time and money [1].

The particularity of underground mines drove many research studies to evaluate the effect of the environment on the link performance. It is well established that propagation characteristics of an underground mine is dependent upon polarization, placement and radiation pattern of the used

Received 18 February 2018, Accepted 24 March 2018, Scheduled 4 April 2018

* Corresponding author: Moulay El Hassan El Azhari (moulay.el-azhari@uqat.ca).

[1] Department of Engineering, UQO, Gatineau, Canada. [2] Department of Engineering, UQAT, Val d'Or, Canada.

antennas [3–5]. With regards to polarization, different studies have reported measurements results on the horizontal, vertical and cross-polarized setups [6–10]. However, for circularly polarized antennas' systems, very few studies are reported on the channel characterization in a tunnel environment and no study has yet been performed in a mine environment. Measurements have been reported in [11, 12], with circularly polarized antennas in railway tunnels with no comparison to linear polarization scenarios. Moreover, these studies mainly focused on the PL and omitted important channel characterization parameters, such as the time dispersion parameters, as well as the channel capacity.

It was experimentally observed that depolarization occurs, in RF transmissions, due to scattering from rough surfaces [13–15]. In fact, it is shown that depolarization from slightly rough surfaces is due to multiple scattering which increase with the roughness of the surface [13]. Instead of it being a disadvantage for linearly polarized antennas, the exploitation of this behavior is possible through the use of circularly polarized antennas. In fact, communication quality could be improved through the polarization diversity [16] Moreover, in the context of the mining environment, depolarization of multipath components occurs and its' degree is dependent upon the relative geometry between the antennas and the scattering object [17]. Since circularly polarized antennas radiate energy in both the horizontal and vertical planes, they exhibit low polarization miss-match losses. Hence, they are expected to mitigate fading, which is generally a problem in underground communications.

Our previous published research works consisted in characterizing the Line-Of-Sight (LOS) underground propagation channel using circularly polarized antennas at 2.4 GHz for a single-input single-output (SISO) system [18, 19]. Channel capacity and PL results were reported. The improvement in the channel capacity and PL exponent through the use of circular polarization was validated. Although the SISO channel capacity was acceptable (with a maximum of 26 bps/Hz for the circular setup and a maximum of 18 bps/Hz for the linear patch setup) for many in-mine applications, the search of higher data rates makes the use of MIMO a trivial choice. Our previous SISO studies did not consider the effect of depolarization on the channel parameters.

In this paper, an in-depth study of the impact of circular polarization on the performance of a MIMO link is performed. Both co-polarized (CP) and cross-polarized (XP) scenarios are considered. The enhancement of the wireless link quality due to circular polarization is proven through a comparison with linearly polarized antenna results. Moreover, the time dispersion properties of the channel and the Rician k-factor are reported and discussed. The channel capacity is derived assuming either a constant transmitted power or a fixed SNR. To the best of the authors' knowledge, no research on MIMO radio channel characterization in underground mines with circularly polarized antenna has been published yet.

The paper is organized in the following manner: Section 2 describes the mine environment, the antennas characteristics, and the measurement setup. In Section 3, experimental results are explained. Finally, in Section 4 the paper is concluded.

2. MEASUREMENT PROCEDURE

2.1. Description of the Underground Mine

Measurements were carried out in a real underground gold mine in Val d'Or-about 530 kilometres north-west of Montreal that is now solely open for tourists and researchers. The gallery is situated at a depth of 90 meters, having a length of approximately 18 m, a height of about 2.45 m and width of approximately 5 m. It is an ideal environment for radio propagation studies. A sketch of the underground gallery and the measurements setup are depicted in Figure 1.

The medium consists essentially of very rough walls and an uneven floor. There are electric wires, cables and pipes attached to the ceiling. The temperature is stable around 8°C, with moisture content near 100% throughout the year. Falling drops of water emerges from the walls and ceiling everywhere and there are puddles of different dimensions on the floor of the gallery. Other elements, such as the mining machinery, ventilation systems and the gratings covering the ceiling contribute to multi-path phenomenon.

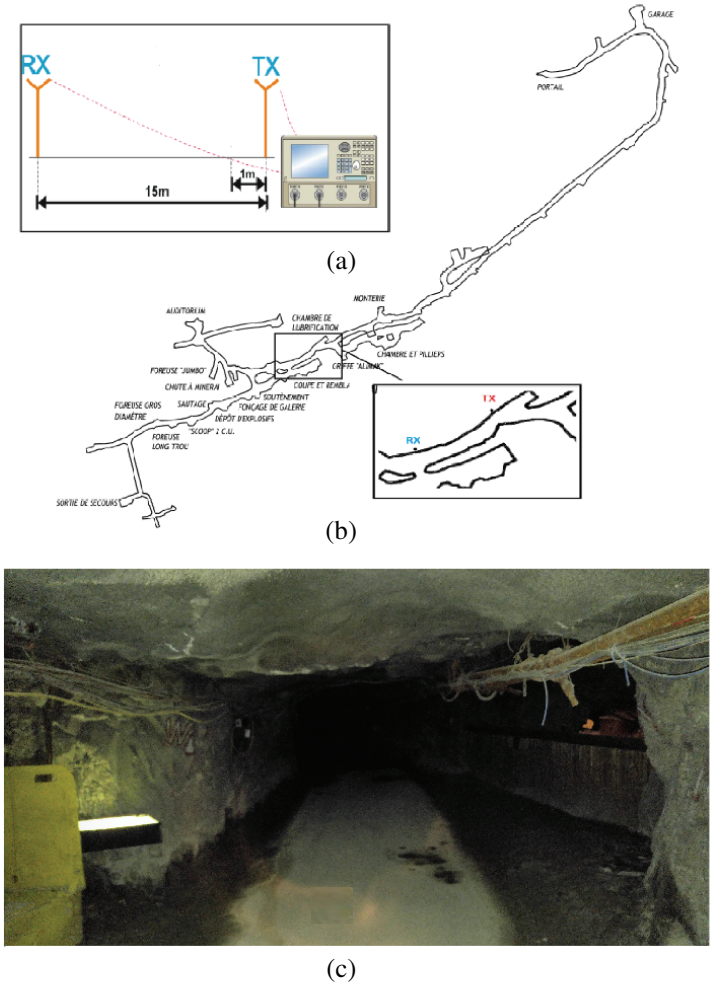

Figure 1. (a) Experiment setup, (b) map of the mine and (c) photo of the gallery.

2.2. Description of the Measurement Setup

Measurements were conducted using two MIMO antenna systems, namely, a 2×2 MIMO circularly polarized patch antenna system and a 2×2 MIMO regular patch antenna system used in previous propagation studies at the LRTCS laboratory [20]. The CP antennas were designed using the High Frequency Structure Simulator (HFSS) antenna design software and fabricated in our laboratory. The two antennas have a gain of 6.6 dBi and an axial ratio (AR) less than 3 dB at 2.4 GHz.

The circularly polarized antennas used an RT 5880 substrate with overall dimension 100 mm (width), 100 mm (length) and 1.6 mm (thickness). Other characteristics consisted of a copper thickness of 0.035 mm, substrate dielectric constant (ε_r) of 2.2 and tangent loss ($\tan\delta$) equaling 0.019. Two symmetric truncated corners (4.2×4.2 mm) on a metal radiator patch cause the antenna to radiate in circular polarity as demonstrated in [21]. The dimensions and the characteristics of the antenna are represented in Figure 2. Since the performance of the Multiple-Input Multiple-Output (MIMO) antenna is quantified through the S-parameters, measurements and simulation results (Figure 2) show that the antenna resonates at the design frequency (2.4 GHz). Moreover, the measured coupling level is found to be about 15 dB within the 2.4 industrial, scientific and medical (ISM) band. Simulation results exhibit a broad 3-dB Axial Ratio (AR) bandwidth of 8.3% (between 2.3 and 2.5 GHz), which covers the WLAN 2.4 GHz operating bands.

The MIMO antennas are separated by a distance of about 7 cm, which is equivalent to half of the wave length ($\lambda/2$). A 30 dB power amplifier is used at the transmission side and a Vector Network

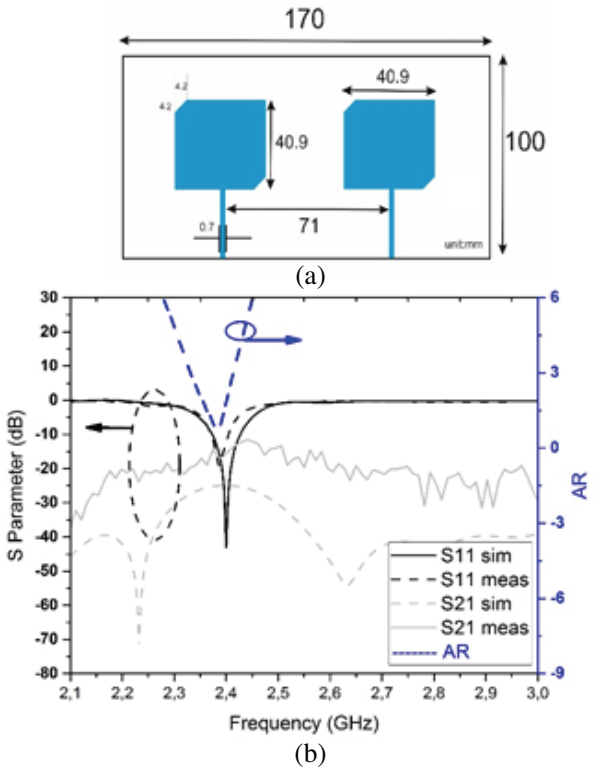

Figure 2. (a) Dimensions of the circularly polarized antenna, (b) simulated (HFSS) and measured S parameters.

Analyzer (VNA) is used to measure the S parameters at the band surrounding the center frequency (2.3 GHz–2.5 GHz). During the measurements, the propagation channel was considered to be stationary; the transmitting and receiving antennas (TX and RX) were fixed on two supporting rods at the same height of 1.50 m. In order to characterize the RF channel, the receiver was moved at 1 m steps from a starting position of 1 m to a final distance of 15 m (from the transmitter) as shown in Figure 1. At each measurement position, 10 snap shots were taken for 2049 frequency points around 2.4 GHz. A description of the measurement parameters is listed in Table 1.

Table 1. Measurement system configurations.

Parameter	Value
frequency	2.3–2.5 GHz
bandwidth	200 MHz
transmitting power	−10 dBm
sweep points	2049
noise floor	−90 dBm
TX gain	6.6 dBi
RX gain	6.6 dBi
cable loss	0.6 dB/m
antenna types	Linearly and circularly polarized patch
antenna height	1.5 m

3. MEASUREMENT RESULTS

3.1. Channel Impulse Response and Path Loss

The impulse response of a wireless channel contains the information necessary to analyze the radio transmission through this channel; it hence characterizes the RF channel. The scattering parameters were measured using a VNA for 2049 frequency points at the 2.3 GHz–2.5 GHz band. An Inverse Fast Fourier Transform (IFFT) is applied to the transfer function (corresponding to the measured S_{21} values averaged over the number of snap shots and antennas) in order to get the impulse responses of the MIMO channel similarly to [20].

Moreover, the power delay profile is directly determined from the impulse response and gives the relative received power as a function of the excess delay. The following formulas represent the MIMO channel and the power delay profile (PDP) respectively [6].

$$Y = HX + N \tag{1}$$

Where X is the $[m \times 1]$ transmitted vector, Y the $[n \times 1]$ received vector, N the receive additive white Gaussian noise (AWGN) vector, and H the $n \times m$ channel matrix.

$$\mathrm{PDP}(t) = \mathrm{mean}(|h(n)|^2) \tag{2}$$

Where $|\cdot|$ is the modulus operation and $h(n)$ is the impulse response.

The bellow graph represents the MIMO impulse responses for both circularly polarized and regular patch antennas at both CP and XP scenarios:

From the above figures (Figures 3–4), it is clear that cross polarization has a significant impact on the linearly polarized setup results. The power of the greatest multipath component, for the regular patch set up, is significantly decreased at the XP scenario compared to the circularly polarized antenna results. This result is expected since the circularly polarized antenna is able to effectively receive signal at both horizontal and vertical direction.

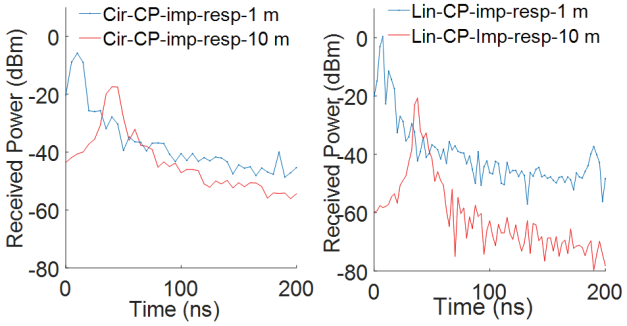

Figure 3. Circular (Cir) and linear (Lin) polarizations impulse responses for two distances at the CP scenario.

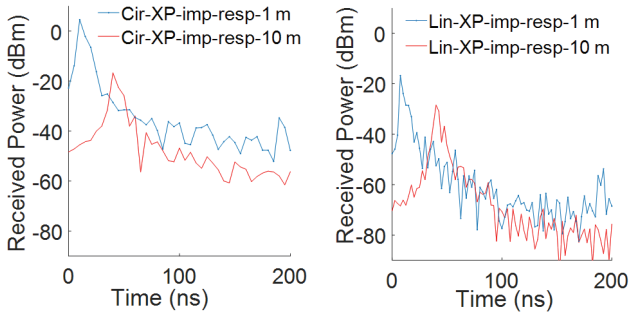

Figure 4. Circular (Cir) and linear (Lin) polarizations impulse responses for two distances at the XP scenario.

The PL-depicted in Figure 5 is a significant link budget component which describes the large-scale effect of the fading channel. It is described by the following formula [6]:

$$PL_{\mathrm{dB}} = 20\log_{10}(\{H_{i,j,f}\}) \tag{3}$$

where PL_{dB} is the PL at a certain position; $H_{i,j,f}$ is the spatial sub-channel path strength (from the ith transmitting antenna to the jth receiving antenna) at a given frequency f; ξ is the averaging operator over all receiving antennas, transmitting antennas, frequencies, and snapshots [6].

A well-known model is used to develop PL as a function of the TX-RX distance d as follows [20]:

$$PL(d) = PL_{\mathrm{dB}}(d_0) + 10\alpha\log_{10}(d/d0) + X \tag{4}$$

where $PL_{\mathrm{dB}}(d_0)$ represents the mean PL at the reference distance d_0, d the distance between the TX and RX, α the PL exponent, and X a zero mean Gaussian variable (in dB) [20].

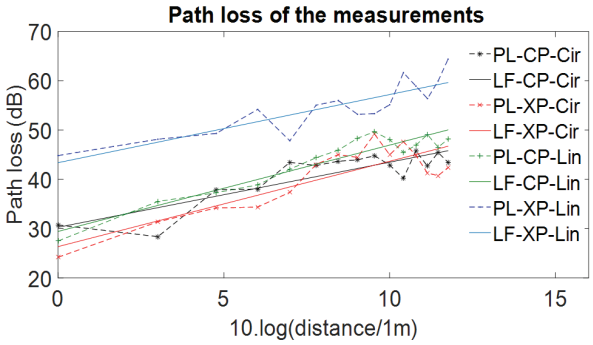

Figure 5. Circular (Cir) and linear (Lin) polarizations PL and linear fitting (LF) at the CP and XP scenario.

Table 2. PL exponent values for the different channel configurations.

Polarization	**Circular**		**Linear**	
Parameters	CP	XP	CP	XP
PL-exponent	1.320	1.731	1.751	1.382
Average shadowing (dB)	0.0008	−0.0016	−0.0002	0.0005
Shadowing STD	2.623	3.423	1.945	2.722

The PL exponent α is smaller than the free-space PL exponent (which is equal to 2) for all the configurations. This is due to the wave guiding effect of the mine gallery [6]. Moreover, the linear regression analysis suggests that the circularly polarized signal decays with a slower rate than the linearly polarized one at the CP configuration. Expectedly, the XP signal for the regular MIMO-patch setup has the worst PL results among all scenarios because of its inherent LOS signal suppression. From the shadowing results, it is clear that the PL values are closer to their linear approximation when linear polarization is used than in the circular polarization case. This is due to the lesser variations around the linear fitting in the case of linear polarization, where the LOS signal is the main contribution to the received power. Compared to the previously published SISO results, it can be observed that the MIMO PL exponents are better than the SISO counterparts [18, 19] due to the MIMO's ability to combat fading. The PL exponent and shadowing results are depicted in Table 2.

3.2. RMS Delay Spread and Coherence Bandwidth

The RMS delay spread is widely used in the characterization of multipath fading channels. It is equal to the square root of the second central moment of the power delay profile (PDP) [22]. The coherence bandwidth (Bc) is directly estimated from the RMS delay spread and measures statistically the range of frequencies over which the channel could be considered flat [22]. From a system design prospective, Bc helps determine whether an equalizer is necessary at the reception [22].

The bellow formulas are used to determine the RMS delay spread and coherence bandwidth (for a frequency correlation function above 0.5).

$$\tau_{RMS} = \sqrt{\bar{\tau}^2 - \bar{\tau}^2} \tag{5}$$

Where $\bar{\tau}$ denotes the mean excess delay and $\bar{\tau}^2$ represents the second moment of the PDP [22].

$$\bar{\tau} = \frac{\sum\limits_k a_k^2 t_k}{\sum\limits_k a_k^2} = \frac{\sum\limits_k p(t_k) t_k}{\sum\limits_k p(t_k)} \tag{6}$$

$$B_c \simeq \frac{1}{5\tau_{RMS}} \tag{7}$$

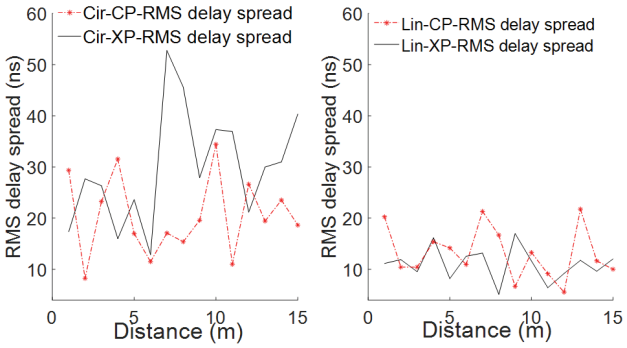

Figure 6. Circular (Cir) and linear (Lin) polarizations RMS delay spread at the CP and XP scenario.

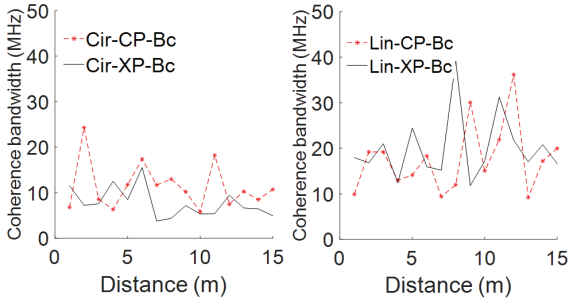

Figure 7. Circular (Cir) and linear (Lin) polarizations coherence bandwidth (Bc) at the CP and XP scenario.

Similarly, to the results reported in [6], the RMS delay spread does not necessarily increase with distance, as shown in Figure 6. It seems that the reflected signals sometimes add constructively and other times destructively for this RF channel resulting in multipath components that do not necessarily increase in number nor in strength as the distance increases. When comparing different polarizations, it is clear that the circularly polarized antenna set up exhibits larger RMS delay spreads and smaller coherence bandwidth (Figure 7) compared to the Linear MIMO setup. This is due to the fact that the circular MIMO set up, which radiates in the horizontal and vertical directions, is able to receive more multipath powers than the linear patch setup. In general, a circularly polarized electromagnetic wave changes its handedness after a reflection from a smooth surface [23]. These first order reflections, which are generally suppressed in a regular tunnel environment, are not suppressed as efficiently in a mine gallery due to the surface roughness [13–15].

3.3. Ricean K-factor

The Rician K-factor is an indication of link quality. It is measured as the relative strength of the direct and scattered components of the received signal, as expressed in the following equation [24]:

$$K(\text{dB}) = 10\log\left(\frac{\varepsilon\,|H|^2}{2var(\,|H|\,)}\right) \tag{8}$$

where ε denotes the mathematical expectation (average), and $var(\cdot)$ refers to the variance of the channel vector H. The K-factor was calculated for each distance between TX and RX, as represented in Figure 8.

The K-factor values do not follow a decreasing trend with distance. In general, the linear MIMO set up at the XP scenario exhibits the lowest k-factor because of the lack of a dominant component (LOS component is effectively suppressed). It is, however observed that even at this scenario (Linear-XP),

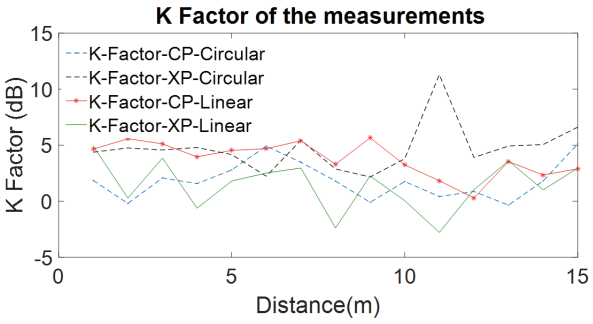

Figure 8. Circular (Cir) and linear (Lin) polarizations K-factor results at the CP and XP scenario.

a certain amount of multipath power is observed due to the surface roughness which causes a signal depolarization. This depolarization makes the cross-polarization less severe; hence a transmission is possible even using the linear MIMO setup at the XP scenario, but with a decreased quality. Moreover, the K-factor is highest for the XP-circular and the CP-linear set ups due to the fact that the LOS component is strongest for these topologies (compared to the multipath signals). Additional statistical K-factor results are represented in Table 3. From this table, it is observed that the K-factor at the Cir-CP is less than that of Lin-CP due to the multipath richness.

Table 3. Statistics of the k-factor for the RF channels inside the mine gallery (Minimum, Maximum, average and standard deviation measured values).

Polarization	**Circular**		**Linear**	
Parameters	CP	XP	CP	XP
k-factor-Average (dB)	1.8561	4.7311	3.8015	1.4313
k-factor-STD (dB)	1.6799	2.1634	1.5293	2.2286

3.4. Channel Capacity

The MIMO channel capacity is usually reported in terms of its CDF [6, 20] or as an average capacity [25]. It depends on two main factors, namely the multipath richness and the PL [20]. In order to explore the effect of the multipath richness on the MIMO channel capacity, a constant signal to noise ratio (SNR) (in our case 20 dB) is assumed [21]. This method isolates the PL from the capacity calculations [21]. Moreover, the PL effect is studied when considering a variable SNR and a constant transmitting power similarly to [21].

MIMO channel capacity is computed using the following formula [21]:

$$C_{\mathrm{MIMO}}[\mathrm{bps/Hz}] = \log_2\left(\det\left[I_n + \frac{\mathrm{SNR}_{av}}{m} HH^*\right]\right) \tag{9}$$

Where I_n is the identity matrix, SNR_{av} the average SNR, H the normalized $m \times n$ channel response, and * signifies the complex conjugate transpose.

The channel capacity results when a constant transmitted power is considered are denoted in Figures 9 and 10. These results show that the average channel capacity decreases with distance. This is explained by the fact that smaller distances correspond to higher received average powers and hence higher average SNRs which has a direct impact on the capacity as given in (9). Moreover, it is observed that the circularly polarized antenna setup generally exhibits higher channel capacities compared to the linear polarization setup for both the CP and the XP configurations. This is due to the suitability

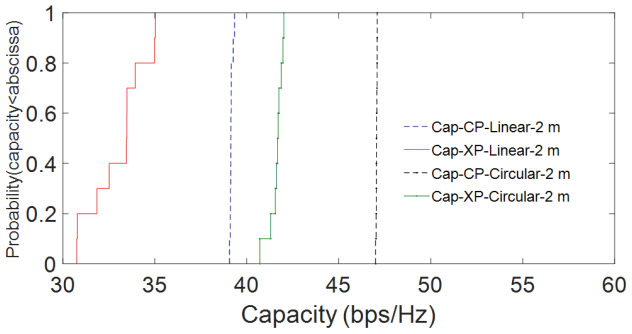

Figure 9. Circular and linear polarizations' MIMO channel capacity CDFs at the CP and XP scenario and a constant transmitted power.

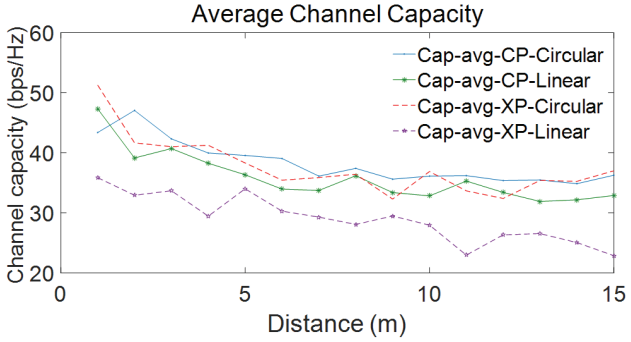

Figure 10. Average MIMO channel capacities at constant transmitted power for Circular and linear polarizations.

of the circular MIMO setup to capture multipath signal at a rough environment. It is observed that the suppression of the reflected wave (for the circular polarization) signals is not performed efficiently due to the rough environment [13–15]. The cross polarized linear MIMO set up exhibits the lowest capacities due to the effective suppression of the LOS signal. The multipath signals still exist, however, due to the additional depolarization caused by the rough surfaces, making the reflected signal visible at the receiver, although with little strength. Expectedly, compared to the previously published SISO results (CP scenarios) [18, 19], the MIMO capacities are considerably higher (more than 1.5 times the SISO capacities).

Figures 11 and 12 show that the channel capacity results at a fixed SNR (20 dB) are very close for all the different configurations. Their values range between 11.1 bps/Hz and 16.7 bps/Hz. Moreover, it is observed that the curves do not follow a monotonic trend, suggesting that the multipath richness is random for these channels. The circularly polarized MIMO setup generally has the highest channel capacities, at the CP scenario, due to its ability to capture multipath signals. The linear setup at the CP scenario and the circular setup at the XP scenario generally exhibit the lowest capacities at an SNR of 20 dB, meaning that these two topologies are least capable to capture the multipath signals. These results are correlated to the K-factor results shown in Table 3.

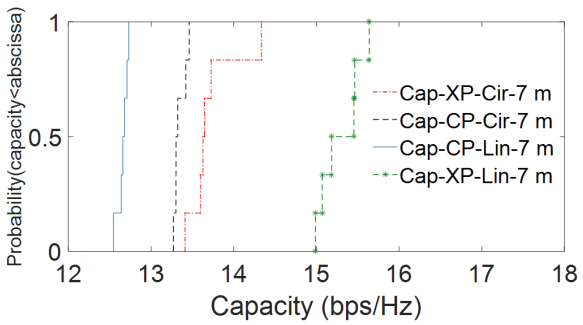

Figure 11. Circular (Cir) and linear (Lin) polarizations MIMO channel capacity CDFs at the CP and XP scenario and a fixed SNR.

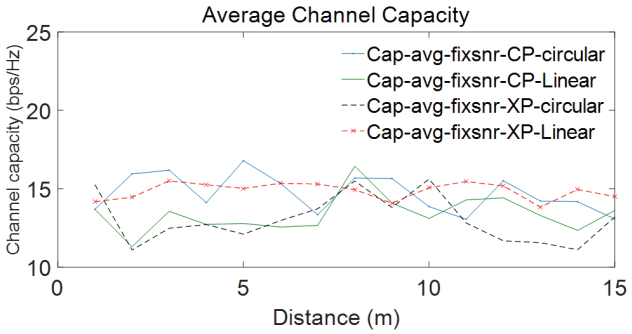

Figure 12. Average MIMO channel capacities at constant SNR for circular and linear polarizations.

4. CONCLUSION

In this paper, the RF channel is characterized at 2.4 GHz in a mine gallery using circularly and linearly polarized MIMO antennas considering CP and XP scenarios. It can be noted that the circularly polarized antennas perform best in a mine environment due to their resilience to cross-polarization.

The PL results for circularly polarized antennas decrease at a low rate for both the CP and XP scenarios, with PL exponents of 1.32 and 1.73, respectively. The linearly polarized setup at the XP scenario has the worst PL values due to the quasi suppression of the LOS signal, which is the strongest multipath component contributing to the total received power. The channel capacity at a constant transmitted power is correlated to the PL results, with channel capacities reaching 51 bps/Hz for the circular-MIMO setup. The results for the channel capacity at a fixed SNR show that the circularly polarized MIMO-CP setup generally has the highest channel capacities due to its ability to capture multipath signals; the MIMO-Lin-CP and the MIMO-Cir-XP setup have the smallest channel capacities (at a fixed SNR) due to their observed limited multipath powers compared to the dominant signal. The channel capacities at a fixed SNR are correlated to the K-factor results. The circularly polarized MIMO setup has the highest RMS delay spread due to the richness of the multipath powers arriving at different time delays. The linear MIMO setup at the XP configurations has the lowest RMS delay spread and a high K-factor due to the limited multipath power reception caused by cross-polarization. Moreover, the surface roughness of the gallery causes a depolarization which helps in the reception (of the reflected signals) at the linear XP topology. This depolarization makes the suppression of the reflected signal for the circular setup inefficient. Hence, a high multipath count is achieved at the circular setup, which further improves the channel capacity.

REFERENCES

1. Forooshani, A. E., S. Bashir, D. G. Michelson, and S. Noghanian, "A survey of wireless communications and propagation modeling in underground mines," *Communications Surveys & Tutorials, IEEE*, Vol. 15, No. 4, 1524, 1545, 4th Quarter, 2013.
2. Mo, L. and Y. Liu, "Underground coal mine monitoring with wireless sensor networks," *ACM Transactions on Sensor Networks*, Vol. 5, Mar. 2009.
3. Sun, Z. and I. F. Akyildiz, "Channel modeling and analysis for wireless networks in underground mines and road tunnels," *IEEE Transactions on Communications*, Vol. 58, No. 6, Jun. 2010.
4. Wang, S., "Radio wave attenuation character in the confined environments of rectangular mine tunnel," *Modern Applied Science*, Vol. 4, No. 2, 65–70, 2010.
5. Huo, Y., Z. Xu, H. D. Zheng, and X. Zhou, "Effect of antenna on propagation characteristics of electromagnetic waves in tunnel environments," *Asia Pacific Conference on Postgraduate Research in Microelectronics Electronics, 2009, Prime Asia 2009*, 268–271, 2009.
6. Mabrouk, I. B., L. Talbi, M. Nedil, and K. Hettak, "MIMO-UWB channel characterization within an underground mine gallery," *IEEE Transactions on Antennas and Propagation*, Vol. 60, 4866–4874, Oct. 2012.
7. Mabrouk, I. B., L. Talbi, and M. Nedil, "Performance evaluation of a MIMO system in underground mine gallery," *IEEE Antennas Wireless Propag. Lett.*, Vol. 11, 830–833, 2012
8. Ghaddar, M., M. Nedil, I. Ben Mabrouk, and L. Talbi, "Multiple-input multiple-output beam-space for high-speed wireless communication in underground mine," *Microwaves, Antennas & Propagation, IET*, Vol. 10, No. 1, 8–15, 2015.
9. Rissafi, Y., L. Talbi, and M. Ghaddar, "Experimental characterization of an UWB propagation channel in underground mines," *IEEE Transactions on Antennas and Propagation*, Vol. 60, No. 1, 240–246, 2012.
10. Benzakour, A., S. Affes, C. Despins, and P. M. Tardif., "Wideband measurements of channel characteristics at 2.4 and 5.8 GHz in underground mining environments," *Vehicular Technology Conference*, 2004.
11. Briso-Rodriguez, C., J. M. Cruz, and J. I. Alonso, "Measurements and modeling of distributed antenna systems in railway tunnels," *IEEE Transactions on Vehicular Technology*, Vol. 56, No. 5, 2870–2879, Sept. 2007.
12. Guan, K., Z. Zhong, J. I. Alonso, and C. Briso-Rodriguez, "Measurement of distributed antenna systems at 2.4 GHz in a realistic subway tunnel environment," *IEEE Transactions on Vehicular Technology*, Vol. 61, No. 2, 834–837, Feb. 2012.
13. Valenzuela, G. R., "Depolarization of E-M waves by slightly rough surfaces," *IEEE Transactions on Antennas and Propagation*, 3rd Edition, Vol. 15, 552–557, 1967.
14. Wright, J. W., "A new model for sea clutter," *IEEE Transactions on Antennas and Propagation*, Vol. 16, 217–223, 1968.
15. Raemer, H. R. and D. D. Preis, "Aspects of parallel-polarized and cross-polarized radar returns from a rough sea surface," *IEEE Trans. on Electromagnetic Compatibility*, Vol. 22, No. 1, 29–44, Feb. 1980.
16. Vaughan, R. G., "Polarization diversity in mobile communications," *IEEE Transactions on Vehicular Technology*, Vol. 39, No. 3, 177–186, 1990.
17. Kwon, S.-C. and G. L. Stuber, "Geometrical theory of channel depolarization," *IEEE Transactions on Vehicular Technology*, Vol. 60, No. 8, 3542–3556, 2011.
18. El Azhari, M. E., M. Nedil, M. Seddiki, N. Kandil, and L. Talbi, "Radio-channel characterization of an underground mine using circularly polarized antennas at 2.4 GHz," *Proc. IEEE Antennas and Propagation Society Int. Symp. (APSURSI)*, Jul. 2017.
19. El Azhari, M. E., M. Nedil, M. Seddiki, N. Kandil, and L. Talbi, "2.4 GHz radio-channel characterization of an underground mine using patch antennas," *Proc. IEEE Antennas and Propagation Society Int. Symp. (APSURSI)*, Jul. 2017.

20. El Azhari, M. E., M. Nedil, I. Benmabrouk, K. Ghanem, and L. Talbi, "Characterization of an off-body channel at 2.45 GHz in an underground mine environment," *Progress In Electromagnetics Research M*, Vol. 43, 91–100, 2015.
21. Yahya, M. and Z. Awang, "Cross polarization ratio analysis of circular polarized patch antenna," *2010 International Conference on Electromagnetics in Advanced Applications*, Sydney, NSW, 442–445, 2010.
22. Rappaport, T. S., "Mobile radiop propagation: Small scale fading and multipath," *Wireless Communications: Principle and Practice*, 2nd Edition, Prentice Hall, 2001.
23. Jackson, J. D., *Classical Electrodynamics*, 3rd Edition, Wiley, New York, 1998.
24. Sarris, J. N. and R. Andrew, "Ricean K-factor measurements in a home and an office environment in the 60 GHz band," *Mobile and Wireless Communications Summit*, *16th IST. IEEE*, 1–5, 2007.
25. Varzakas, P., "Average channel capacity for rayleigh fading spread spectrum MIMO systems," *International Journal of Communication Systems*, Vol. 19, No. 10, 1081–1087, Dec. 2006.